

mPEG-NHS carbonates: Effect of alkyl spacers on the reactivity: Kinetic and mechanistic insights

Victoria A. Vaillard, Malen Menegon, Nicolás I. Neuman, Santiago E. Vaillard 

Instituto de Desarrollo Tecnológico para la Industria Química (INTEC). CCT Santa Fe CONICET-UNL, Colectora Ruta Nacional 168, Km 472, Paraje "El Pozo" (3000), Santa Fe, Argentina

Correspondence to: S. E. Vaillard (E-mail: svaillard@intec.unl.edu.ar)

ABSTRACT: Nowadays, the chemical conjugation to mPEG, also known as PEGylation, is a well-recognized technology used to improve the pharmaceutical properties of the therapeutic proteins. Over the last 20 years, more than 10 PEGylated macromolecules reached the market with tremendous success, whereas various other bioconjugates are under advanced clinical trials. mPEG-*N*-hydroxysuccinimidyl carbonate is an important reagent of widespread application for the PEGylation of biomacromolecules. One of the most important challenges in this technology is the development of more selective PEGylation reagents aimed to provide more consistent polymer-protein conjugates. One approach followed to improve the selectivity of PEGylation reagents is the design of less reactive derivatives, for example, by incorporation of alkyl spacers between the polymer chain and the terminal reactive group. In this work, we prepared a family of mPEG-*N*-hydroxysuccinimidyl carbonates bearing spacers of up to 6 carbon atoms. The kinetics of hydrolysis of the carbonates was studied under different experimental conditions, as a straight measure of the influence of the length of the spacer on the reactivity. By DFT calculations, we propose a detailed mechanism for the hydrolysis reaction. The influence of the length of alkyl spacer on the reactivity of the carbonates and related esters is studied and discussed in detail. Finally, to further evaluate the reactivity, selected *N*-hydroxysuccinimidyl carbonates were studied in the conjugation reaction of bovine lactoferrin. © 2018 Wiley Periodicals, Inc. *J. Appl. Polym. Sci.* **2018**, *135*, 47028.

Received 4 April 2018; accepted 15 July 2018

DOI: 10.1002/app.47028

INTRODUCTION

Since the FDA approved the first PEGylated product in the early 90s, the covalent attachment of mPEG to peptides and proteins has been of outstanding relevance for the biopharmaceutical industry. This technology, known as PEGylation, is used to improve the biopharmaceutical properties of several macromolecules, which enabled a new generation of more effective and safer biopharmaceuticals. The economic impact of this technology shows a sustained increase over the years, and it is expected that the market share of PEGylated drugs in Europe and the United States only could reach as much as 10 billion by year 2024.

Acylation reactions of $-NH_2$ groups using *N*-hydroxysuccinimide (NHS) esters **1** (Figure 1) and carbonate ester **2** (Figure 1) are reliable methods to achieve peptide and protein PEGylation. Thus, although reagent **1** affords amide protein-polymer bonds, carbonate **2** provides stable urethane linkages.^{1,2} It is noteworthy that these chemistries have found widespread application in academia and industry to obtain bioconjugates with improved pharmacokinetic profiles.^{3–9}

To be useful in PEGylation by acylation reactions, any given acylating reagent should present a good balance between its reactivity

with proteins and its stability toward hydrolysis. For example, mPEG-NHS acetate (compound **1a**, Figure 1) is so reactive that it usually affords undesirable high degrees of the hydrolyzed polymer and poly-PEGylated adducts, compromising the purification of the required mono-PEGylated biomacromolecule, and limiting the utility of this reagent. It has been reported that the introduction of an aliphatic spacer of more than 2 carbon atoms between the polymer chain and the terminal carboxylate-NHS ester group, increases the stability of mPEG-NHS carboxylates.¹⁰ The trend is that as the length of the spacer increases, the reactivity decreases, or the stability increases upon hydrolysis of the reactive polymer.¹⁰ In fact, kinetic data for the hydrolysis of esters **1** have been published and used as a measure of the reactivity of mPEG-NHS esters.^{11,12} However, despite of this widely accepted tenet, an explanation for this phenomenon has so far not been provided. In any case, it is nowadays well accepted that mPEG-NHS propionate and butyrate (compounds **1b** and **1d**, respectively, Figure 1) are less reactive than mPEG-NHS acetate, making them more useful PEGylating reagents because the use of excessive amounts of mPEG reagents needed to surpass instability under aqueous conditions can lead not only to unwanted over-PEGylation of the target protein but also to serious

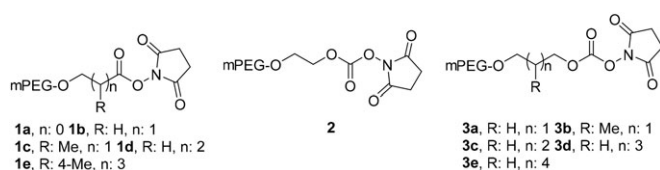


Figure 1. mPEG–NHS esters **1** and NHS carbonate esters **2** and **3**.

difficulties in the purification of the conjugates. A similar reactivity pattern has been proposed for mPEG–aldehydes (acetaldehyde, propionaldehyde, and butyraldehyde), which are used for site-selective conjugation by the reductive amination process.

mPEG–NHS carbonate **2** is structurally different from esters **1**, affording urethane polymer–protein linkages instead of amide bonds. Although **2** is one of the most used reagents in PEGylation technology, it has some drawbacks related to its reactivity and instability in aqueous alkaline medium. Probably, because of the lack of suitable synthetic intermediates, the introduction of aliphatic spacers of more than 2 carbon atoms, as a means of reducing the reactivity of compound **2**, has not previously been investigated.

The in-depth knowledge about the reactivity of mPEG–NHS carbonates should enable a more rational design of the conjugation reactions, in such a way as to allow decreasing unwanted secondary competing reaction, which should simplify the subsequent demanding and expensive purification steps.

In this work, we introduce a simple method for synthesis of mPEG–NHS carbonates bearing spacers of up to 6 carbon atoms (compounds **3a–e**, Figure 1), which have not previously been reported. Compounds **3a–e** are designed to provide PEGylation reagents with tuned reactivity. A detailed kinetic study of the hydrolysis reactions of the carbonates **3** is also presented and discussed. The mechanism of the hydrolysis reactions was studied by DFT calculations, and an explanation for the effect of the lengths of the spacer linker on the stability is proposed for these materials and for relevant esters **1**. In light of the results of the hydrolysis experiments and to further evaluate the reactivity, selected carbonates **2** and **3a** were evaluated in the bioconjugation of bovine lactoferrin (bLF) as model protein.

EXPERIMENTAL

Materials

mPEG of 12 and 20 kDa size and mPEG–NHS carbonate **2** of 5 kDa size (>95% in all cases) were all obtained from JenKem Technology (Allen, TX, USA). *N,N'*-Disuccinimidyl carbonate (>98%) and NHS (>98%) were supplied by Sigma-Aldrich (Sigma-Aldrich de Argentina, Ciudad Autónoma de Buenos Aires, Argentina). The hydroxyl-terminated polymers **4** were obtained by substitution reaction of mPEG-mesylate with monoalkoxides of symmetrical diols, following a method published by our group.¹³ Pyridine, dichloromethane, and acetonitrile (HPLC grade) were distilled and stored over molecular sieves (4 Å). bLF (99% purity, with a molecular weight of approximately 80 kDa) was obtained from Master Pharm (Lodz, Poland) and used without further purification. All other reagents and solvents were used as received from the suppliers.

Physicochemical Characterization and Analyses

¹H NMR experiments were performed in CDCl₃ in a Bruker Avance II 300 MHz spectrometer and referenced to the residual solvent signal. Signal suppression experiments (for the repetitive oxyethylene unit) were performed using Bruker WATERSUP pulse sequence with an o1p at 3.659 ppm. FTIR spectra were obtained with Shimadzu FTIR-8201 PC apparatus. UV–vis analyses were performed on a Shimadzu UV–vis spectrophotometer. MALDI-TOF data were obtained at Centro de Estudios Químicos y Biológicos por Espectrometría de Masa (CEQUIBIEM) from Universidad de Buenos Aires (FCEN-UBA Argentina). ¹H NMR, FTIR, and MALDI-TOF spectra are provided in the Supplementary Information accompanying this article.

Synthesis of mPEG–NHS Carbonates **3** from Hydroxyl-Terminated mPEGs **4**

mPEG–NHS carbonates were obtained following a modified procedure. To a dry 50 mL Schlenk tube equipped with a magnetic stirrer were added mPEG–OH or mPEG alcohol **4** (1 equiv, 0.025 mmol) and 4 mL of dichloromethane under nitrogen at room temperature. Then, 20 equiv *N,N'*-disuccinimidyl carbonate was added as a suspension in acetonitrile (128 mg, 0.50 mmol in 2 mL of solvent), followed by addition of dry pyridine (10 equiv, 20 μL). After 30 min, a new portion of pyridine was added (40 equiv, 80 μL). The reaction was maintained with stirring at room temperature overnight. The mixture was transferred to a 50 mL Falcon tube, and the solvent was evaporated to reach approximately 5 mL and then precipitated with cold diethyl ether (40 mL). The tube was centrifuged for 10 min at 4000 rpm. The ethereal phase was separated, and the solid was dissolved in dichloromethane (5 mL) and reprecipitated. The process was repeated three additional times, and the solid was dried under vacuum. The same procedure, but using mPEG–OH, was followed to obtain carbonates **2** of 12 and 20 kDa size. All products were obtained with high purity (>95%, checked by ¹H NMR) as white solids. Carbonates were characterized by FTIR, MALDI-TOF, and ¹H NMR. Yields are expressed as % of recovered polymer masses, and the degrees of activation (% of conversion of –OH to NHS carbonate) were determined by UV spectrophotometry.

mPEG–NHS carbonate **2** of 12 kDa size (83%, 252 mg, 92% of activation). ¹H NMR (CDCl₃) δ: 2.84 (bs, 4H, succinimidyl ring); 3.37 (s, 3H, CH₃O–); 3.40–3.94 (m, mPEG chain); 4.14–4.47 (m, 2H, –CH₂–OCOO–NHS).

mPEG–NHS carbonate **2** of 20 kDa size (94%, 473 mg, 100% of activation). ¹H NMR (CDCl₃) δ: 2.84 (bs, 4H, succinimidyl ring); 3.37 (s, 3H, CH₃O–); 3.39–3.94 (mPEG chain); 4.40–4.47 (m, 2H, –CH₂–O–CO–O–).

mPEG–NHS carbonate **3a** of 20 kDa size (99%, 500 mg, 73% of activation). ¹H NMR (CDCl₃) δ: 2.86 (bs, 4H, succinimidyl ring); 3.39 (s, 3H, CH₃O–); 3.39–3.94 (mPEG chain); 4.40–4.47 (m, 2H, –CH₂–O–CO–O–).

mPEG–NHS carbonate **3b** of 20 kDa size (62%, 313 mg, 83% of activation). ¹H NMR (CDCl₃) δ: 1.00 (d, *J* = 6.95 Hz, 3H, CH₂–CH[CH₃]–CH₂); 1.24–1.25 (m, 4H); 2.84 (bs, 4H, succinimidyl ring); 3.38 (s, 3H, CH₃O–); 3.39–3.91 (m, mPEG chain); 4.22–4.38 (2 × dd, 2H, diastereotopic –CH₂–O–C[O]–O).

mPEG-NHS carbonate **3c** of 20 kDa size (95%, 480 mg, 88% of activation). $^1\text{H NMR}$ (CDCl_3) δ : 1.53–1.57 (m, 2H); 1.60–1.69 (m, 4H); 2.84 (bs, 4H, succinimidyl ring); 3.38 (s, 3H, CH_3O); 3.39–3.96 (m, mPEG chain). 4.28–4.37 (m, 2H, $-\text{CH}_2-\text{OCOO}-\text{NHS}$).

mPEG-NHS carbonate **3d** of 20 kDa size (77%, 389 mg, 73% of activation). $^1\text{H NMR}$ (CDCl_3) δ : 0.80–0.88 (m, 8H); 2.83 (bs, 4H, succinimidyl ring); 3.36 (s, 3H, CH_3O); 3.40–3.94 (m, mPEG chain); 4.28–4.33 (m, 2H, $-\text{CH}_2-\text{OCOO}-\text{NHS}$).

mPEG-NHS carbonate **3e** of 20 kDa size (69%, 349 mg, 89% of activation). $^1\text{H NMR}$ (CDCl_3) δ : 1.23–1.25 (m, 2H); 1.38–1.42 (m, 4H); 1.59–1.61 (m, 4H); 2.84 (bs, 4H, succinimidyl ring); 3.37 (s, 3H, CH_3O); 3.40–3.94 (m, mPEG chain); 4.27–4.34 (m, 2H, $-\text{CH}_2-\text{OCOO}-\text{NHS}$).

In all cases, FTIR analyses revealed three peaks corresponding to succinimidyl ring and carbonate functionalities ($\text{C}=\text{O}$ absorptions, 1850–1650 cm^{-1}).

Degree of Activation of Polymers **3a–e** by UV Spectrophotometry

The degrees of activation were measured by quantification at 260 nm of the NHS anion released after hydrolysis of carbonates under alkaline conditions (NH_4OH , 0.1 N). An ϵ of 7819 $\text{M}^{-1} \text{cm}^{-1}$ was obtained for the calibration curve using solutions of known concentrations of NHS under identical experimental conditions.

A sample of carbonate (of approximately 5 mg in 0.1 mL of acetonitrile) was added to 2 mL of NH_4OH (0.1 N), and the solution was homogenized three times. After incubation at room temperature for 5 min, the absorbance of the sample was measured at 260 nm.

Kinetics of Hydrolysis of mPEG-NHS Carbonate **3a–e** under Alkaline Conditions

All determinations were made at 25°C following the same methodology but varying the nature of buffer solutions. For each buffer, the ϵ of NHS anion was determined by the calibration curve method. For all carbonates, pseudo-first-order kinetics with respect to carbonate concentration was found. Carbonate ester concentrations were determined indirectly by measurement of concentration of NHS anion. A solution of carbonate was prepared in acetonitrile (~5 mg in 0.1 mL) and added to 2 mL of buffer, homogenized, and immediately analyzed by UV spectrophotometry (kinetic mode, measurements every 10 seconds) at 260 nm. Kinetic data provided in Tables I and II are the results of at least three different experiments.

Bioconjugation Reaction of Carbonate Esters **2** and **3a** to bLF

PEGylation reactions were carried out in 50 mM phosphate buffer, pH 8.00, at 25°C for 24 h and stopped by addition of SDS-PAGE loading buffer. The bLF final concentration was 1 mg/mL, and 20 kDa mPEG carbonates **2** and **3a** were added in a molar ratio of 1:1. PEGylation reaction mixtures were analyzed by SDS-PAGE using 7.5% polyacrylamide under nonreducing conditions. After running, gels were rinsed with distilled water and placed in a 5% barium chloride solution. The gels were maintained for 10 min with gentle mixing, and then they were

Table I. Values of $\tau_{1/2}$ (min) of Alkaline Hydrolysis for mPEG-NHS Carbonate Esters **2** and **3a–e** in Borate Buffer

Entry	Polymer	pH 8.0, 0.1 M	pH 9.0, 0.1 M	pH 8.0, 0.2 M
1	2^a	51 ± 4	5.8 ± 0.4	44 ± 4
2	2^b	49 ± 3	6.2 ± 0.9	40 ± 4
3	2^c	44 ± 2	5.5 ± 0.6	44 ± 4
4	3a	140 ± 14	13 ± 1	132 ± 13
5	3b	89 ± 8	12 ± 1	93 ± 9
6	3c	118 ± 10	14 ± 1	118 ± 3
7	3d	90 ± 9	17 ± 1	103 ± 3
8	3e	104 ± 10	15 ± 1	120 ± 10

^a 5 kDa.

^b 12 kDa.

^c 20 kDa.

rinsed again and placed in a 0.1 N I_3^- solution for 5 to 10 min. In the case of proteins or PEG-protein conjugates, standard staining procedures with Coomassie Brilliant Blue were followed. Both gels were analyzed by ImageJ software.

DFT Calculations

DFT electronic structure calculations were performed with the ORCA program package.¹⁴ The Perdew–Burke–Ernzerhof functional was used with a def2-TZVP basis set,^{15,16} an auxiliary def2/J basis for density-fitting resolution of the identity, geometric counterpoise correction,^{17,18} atom pairwise dispersion with Becke–Johnson damping (D3BJ),^{19,20} and solvation using the conductor-like continuum polarizable model (CPCM) model as implemented in ORCA 4.0.²¹

RESULTS AND DISCUSSION

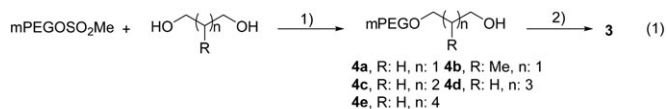
Synthesis and Characterization of mPEG Carbonates Bearing Aliphatic Spacers

PEGylation of $\epsilon\text{-NH}_2$ group of lysine amino acids using activated mPEG carbonate esters and related compounds has vastly been exploited in bioconjugation technology. Among the various reagents that have been used to obtain stable polymer–protein urethane linkages, most of the attention has been centered on mPEG carbonate **2**, which in fact is commercially available. NHS esters of mPEG–carboxylic acids **1** (Figure 1) are also well-known reagents, which have found application in the conjugation of

Table II. Values of $\tau_{1/2}$ (min) of Alkaline Hydrolysis for mPEG-NHS Carbonates **2** and **3a–e** in Phosphate Buffer

Entry	Polymer	pH 8.0, 0.1 M	pH 8.0, 0.5 M
1	2^a	40 ± 3	8 ± 1
2	3a	110 ± 9	41 ± 4
3	3b	98 ± 5	36 ± 4
4	3c	136 ± 7	26 ± 3
5	3d	117 ± 4	41 ± 4
6	3e	131 ± 4	36 ± 3

^a 20 kDa.



1) NaH/DMF/80 °C. 2) bis-NHS-carbonate/Et₃N/RT

Figure 2. Synthesis of mPEG–NHS carbonates **3a–e**.

several different proteins. In clear contrast with esters **1**, the influence of length of the spacer on the reactivity and stability of important carbonate esters of the type of **3** (Figure 1) has not previously been investigated, probably due to the lack of a method for the synthesis of these reactive polymers. Recently, we have developed a simple and straightforward strategy for the synthesis of mPEG–alkyl aldehydes and carboxylic acids.¹³ The key synthetic intermediates of the method are hydroxyl-terminated mPEGs **4** [Figure 2, eq. (1)], which were converted to the target polymers by oxidative reactions. With key hydroxyl polymers **4a–e** in hand from our previous work, we decided to extend the utility of these materials to the synthesis of carbonates **3**. After some experimentation, we found that alcohols **4a–e** were cleanly converted to the required ester carbonate **3a–e** (Figure 3) when the reaction was performed in a dichloromethane–acetonitrile solvent mixture using pyridine as base.²² After simple precipitation workup to eliminate low-molecular-weight impurities, high yields of mPEG carbonates **3a–e** were obtained (Figure 3, 62–99%). Following the same methodology, carbonates **2** from mPEG of 12 and 20 kDa size were obtained in excellent yields (83 and 94%, respectively). It is worth mentioning that toxic phosgene of triphosgene was not needed to obtain high yields of the target carbonates.^{23,24}

All new carbonates **3a–e** were characterized by FTIR and ¹H NMR, as presented for **3a** in Figures 4 and 5, respectively (see Supporting Information for carbonates **2** and **3b–e**). FTIR clearly showed a C=O stretching band in the 1850–1650 cm⁻¹ region. For comparative purposes, the FTIR of a commercial sample of **2** of 5 kDa size, together with **2** of the same molecular weight but obtained using the method presented herein, is also included in Figure 4(b).

As expected, ¹H NMR showed a NHS proton signal at around 2.80 ppm, together with terminal –OCH₃ at around 3.34 ppm and a signal at around 4.40 ppm, which is assigned to –CH₂–OCO– protons (Figure 5). Integration of terminal –OCH₃ and NHS ring protons suggested that the conversion of **4a** to **3a** was complete. Full spectral data for all synthesized carbonates (¹H NMR, FTIR, and MALDI-TOF) together with the assignment of signals are provided in the Supporting Information accompanying this article. As an example, MALDI-TOF of **3a** is presented

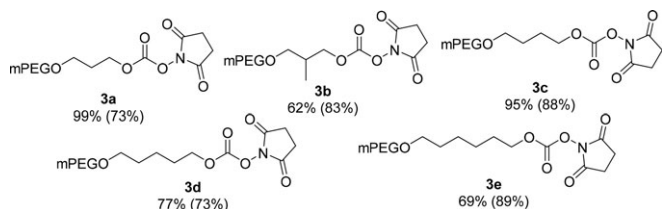


Figure 3. mPEG carbonates **3a–e**. Degree of activation by UV spectrophotometry indicated in parenthesis.

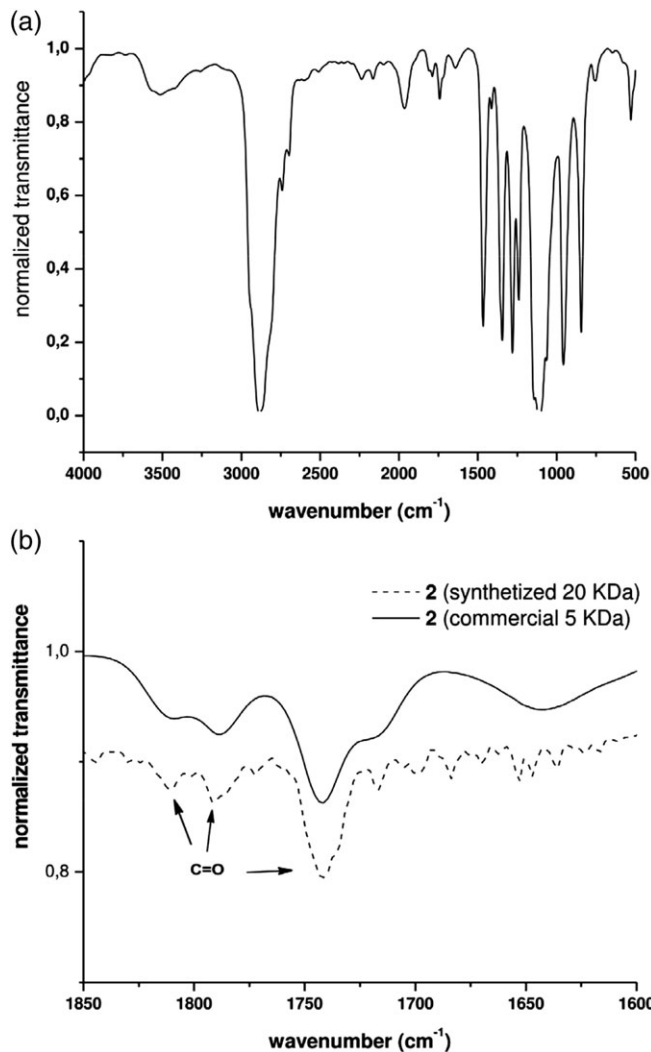


Figure 4. (a) FTIR spectrum of carbonate ester **3a**. (b) FTIR spectrum of carbonate ester **2** of 5 kDa size (commercial sample) and **2** of 20 kDa size (synthesized sample), C=O stretching region.

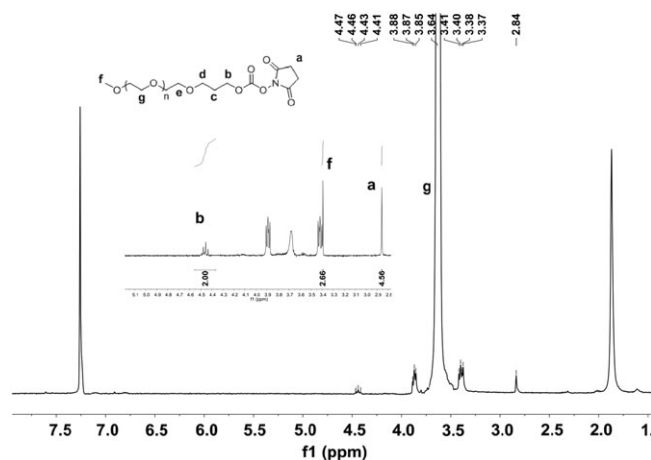


Figure 5. ¹H NMR (CDCl₃, 300 MHz) for **3a** and ¹H NMR spectra, with suppression of chain signal of mPEG.

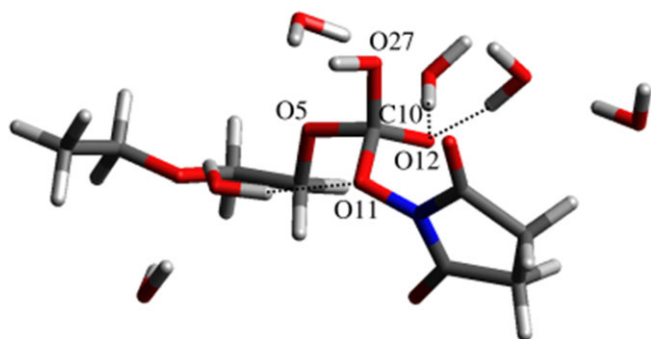


Figure 8. Optimized structure of the tetrahedral intermediate involved in hydroxide ion nucleophilic attack to the carbon atom of the carbonate. Dashed lines indicate hydrogen bonds, which help to stabilize the tetrahedral intermediate. [Color figure can be viewed at wileyonlinelibrary.com]

all polymers when the ionic strength is increased to 0.5 M at the same pH. This result would be assigned to a solvation effect, which would make the reactions faster.

The increase in reaction rate with the increase of ionic strength is indicative of a mechanism in which a charged tetrahedral intermediate is formed upon attack to the carbonate carbon atom by a hydroxide ion. DFT geometry optimization of this tetrahedral intermediate supports this mechanism. Figure 8 shows the structure of the optimized tetrahedral intermediate for a truncated form of **2a**, with selected atom labels. Table III shows the partial Mulliken atomic charges and selected bond distances and angles. Numerical frequency calculations show no imaginary frequencies, thus indicating that the structure is a local minimum.

The presence of a tetrahedral intermediate with a net negative partial charge, particularly, on the carbonyl oxygen atom (O12), explains why a higher ionic strength increases reaction rates for all compounds. The presence of the buffer cations (Na^+) helps to stabilize the negative charge of the intermediate.

Fox and coworkers have discussed different mechanisms for nucleophilic substitution on carbonyl carbon atoms by DFT methods.²⁸ It has been pointed out that the formation of a tetrahedral intermediate requires extensive solvation of the carbonyl oxygen (O27 in our molecular model). Therefore, the results obtained here agree with the mechanism proposed by these authors for the nucleophilic attack of methyl acetate with a methoxide ion.

The kinetics of hydrolysis of compounds **2a** and **3a–e** shows variations in the same order of magnitude, suggesting that the same

Table III. Partial Mulliken Atomic Charges and Selected Bond Distances and Angles

Atoms	Atomic charges	Bond distances	Å	Bond angles	°
C10	0.394	C10–O5	1.436	O5–C10–O11	100.3
O5	–0.257	C10–O11	1.549	O5–C10–O12	119.1
O11	–0.404	C10–O12	1.284	O5–C10–O27	104.1
O12	–0.495	C10–O27	1.502	O11–C10–O12	113.5
O27	–0.521 (–0.181) ^a	-	-	O11–C10–O27	103.4
-	-	-	-	O12–C10–O27	114.4

^a The H atom charge was added to the O27 atom charge.

Table IV. Solvation Energies for Carbonates **2** and **3a–e** and for Esters **1a–e**. Dimerization Energies for Carbonates **2** and **3a**

Polymer	Solvation energy (Ha)	Solvation energy (kcal/mol)	Solvation energy/non-H atom (kcal/mol)
2	–0.0332	–20.839	–1.3024
3a	–0.0307	–19.268	–1.1334
3b	–0.0300	–18.826	–1.0459
3c	–0.0303	–19.040	–1.0578
3d	–0.0293	–18.362	–0.9664
3e	–0.0316	–19.812	–0.9906
1a	–0.0239	–14.997	–1.075
1b	–0.0225	–14.119	–0.9440
1c	–0.0213	–13.366	–0.8370
1d	–0.0229	–14.370	–0.900
1e	–0.0224	–14.056	–0.826
	Dimerization energy (Ha)	Dimerization energy (kcal/mol)	
2	–0.0144	–9.036	
3a	–0.0186	–11.672	

mechanism operates in all cases, precluding a rationalization of the variations in the reaction rates through calculation of activation energies by DFT methods. The experimental rate constants for the different compounds correlate with very small differences in activation energies, far below the expected precision of the computational approach used herein. Instead, these small differences suggest that the changes in the reactions rates are caused by conformational or other subtle effects. As the structural differences between compounds **2** and **3a–e** appear only after the β carbon of the carbonate group, variations in the rate of nucleophilic attack due to the steric hindrance introduced by the spacer seem unlikely and cannot account for the indicated rate differences. Another possibility to explain these differences is the formation of transient aggregates due to the varying hydrophobic nature of the alkyl spacers. To probe this possibility, we calculated the solvation energies for the truncated forms of compounds **2** and **3a–e**, with formulas $\text{C}_2\text{H}_5\text{–O–R–OCO}_2\text{–NHS}$ [**2**: $\text{R} = \text{–C}_2\text{H}_4\text{–}$, **3a**: $\text{R} = \text{–C}_3\text{H}_6\text{–}$, **3b**: $\text{R} = \text{–CH}_2\text{–CH(CH}_3\text{)–CH}_2\text{–}$, **3c**: $\text{R} = \text{–C}_4\text{H}_8\text{–}$, **3d**: $\text{R} = \text{–C}_5\text{H}_{10}\text{–}$, **3e**: $\text{R} = \text{–C}_6\text{H}_{12}\text{–}$], using the CPCM solvation model as implemented in ORCA 4.0 [Table IV and Figure 9(a)].¹⁶ As the solvation energy increases (in absolute value, all else being equal) with the number of atoms due to

dispersive forces, we also calculated the solvation energies per non-H atom. For each molecule, we performed separate gas-phase and solvated geometry optimizations. As indicated earlier, kinetic data for the hydrolysis of mPEG-carboxylic acid NHS esters bearing aliphatic spacers is well known in PEGylation chemistry. Despite this, information is routinely invoked as a rule of thumb for selection of any given mPEG-NHS ester, a rational explanation to describe the influence of the alkyl spacer length on the reactivity of this important family of compounds has so far not been provided. Therefore, for comparison purposes, we also calculated the solvation energies for the related mPEG-carboxylic acid NHS esters **1** (Figure 1, **1a**: mPEG-acetic acid, **1b**: mPEG-propionic acid, **1c**: mPEG-2-methylpropionic acid, **1d**: mPEG-butyric acid, and **1e**: mPEG-4-methylbutyric acid). These results are also presented in Table IV and Figure 9(b). Whereas a clear and nearly linear increase (i.e., less negative values) in solvation energies, with the increase in the number of carbon atoms in the alkyl spacer, is observed for esters, there is an increasing but more dispersed tendency for carbonates. The increasing hydrophobicity (evidenced by a decrease in absolute value of the solvation energy per non-H atom) for esters correlates with the increase in the hydrolysis half-lives. This suggests that, indeed, local hydrophobicity could play a role in the hydrolysis rates, with an increase in hydrophobicity, probably by favoring the formation of transient aggregates, which decrease the ester availability toward hydrolysis. For the carbonates studied in this work, this tendency is less clear, with the solvation energy per non-H atom increasing in a nonmonotonic way with the number of carbon atoms in the spacer. This actually is congruent with the

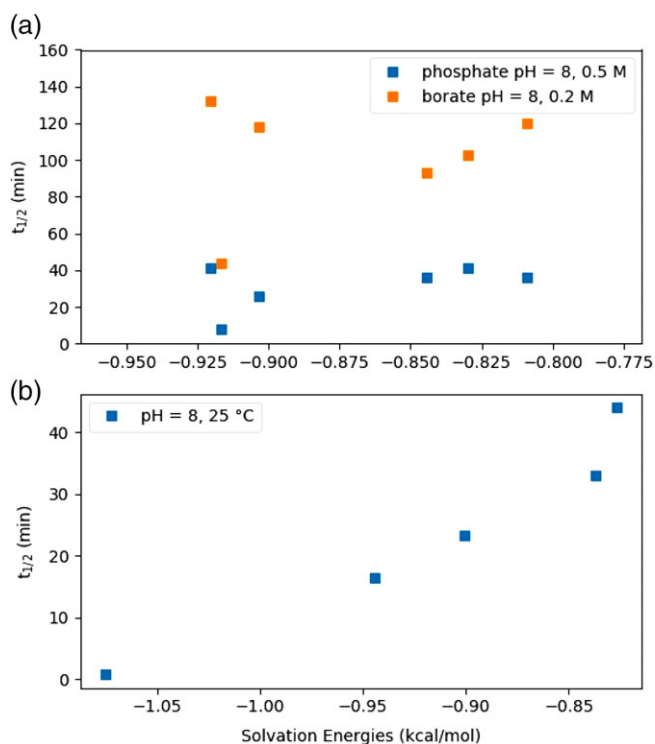


Figure 9. Hydrolysis half-lives vs solvation energies per non-H atom for the series of (a) carbonates **2** and **3a–e** and (b) esters **1a–e**. [Color figure can be viewed at wileyonlinelibrary.com]

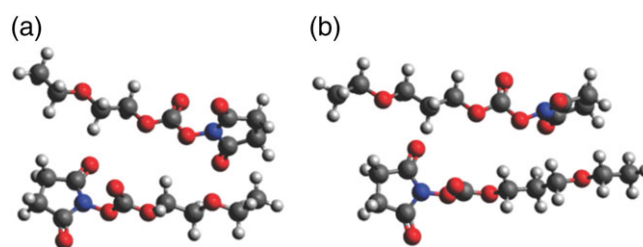


Figure 10. Molecular structures of dimers of truncated forms of (a) **2** and (b) **3a**. [Color figure can be viewed at wileyonlinelibrary.com]

dispersion in the hydrolysis half-lives for the studied carbonates under various buffered conditions. A possible explanation is that the carbonates contain two more atoms (a carbon atom and an oxygen atom) between the first oxyethylene unit of PEG oxygen and the carbonate carbon atom, compared to esters in the same series, which probably allows for a larger conformational freedom for the former compounds. However, as for carbonates, the largest difference in hydrolysis rates is observed between **2** and **3a**; we decided to calculate explicitly the dimerization energies. These results are also shown in Table IV, and the structures of the optimized dimers are shown in Figure 10.

The differences in the solvation energies between **2** (ethyl spacer) and **3a** (propyl spacer) are relatively small (less than 7%), but the dimerization energies for these two polymers are more significantly different (25%). This finding supports the idea of transient aggregate formation, which may reduce steric availability of the carbonate group toward nucleophilic substitution by hydroxide ions. The increase in the length of the alkyl spacer seems to have a larger effect regarding dimer formation than it does relative to solvation energy, in contrast with the results obtained for esters **1**.

PEGylation to bLF

Given the significant differences found in the rates of hydrolysis of carbonates **2** and **3a** and with the aim of evaluating if this effect translates into the modification of the outcome of a PEGylation reaction, these reagents were further studied in the conjugation of bLF. bLF is a well-known tetrameric transferrin with a molecular weight of around 80 kDa. The biological activity of bLF is also well documented.^{29–32} Linear mPEG-*p*-nitrophenyl carbonate of 20 kDa size has been used for the bioconjugation of this protein. The effect of pH on the yield of mono-PEGylated products, as well as the effect on the stability of the reagent, has both been studied in detail.³³ In a series of works, Sato and coworkers employed 20 and 40 kDa linear and branched mPEG for the conjugation of bLF. The chemistry of these last conjugations involved the formation of amide linkages using mPEG-NHS esters. The conjugates were evaluated in formulations for oral administration and for their hepatoprotective capacities against acute injury by carbon tetrachloride and galactosamine.^{34–38}

We performed the PEGylation of bLF with reagents **2** and **3a** in phosphate buffer at pH 8.0 using a protein/mPEG molar ratio of 1:1. To evaluate the evolution of the conjugation reactions, samples were taken at different reaction times and run in SDS-PAGE experiments (Figure 11). After staining and rinsing with water, the gels were analyzed using ImageJ software.

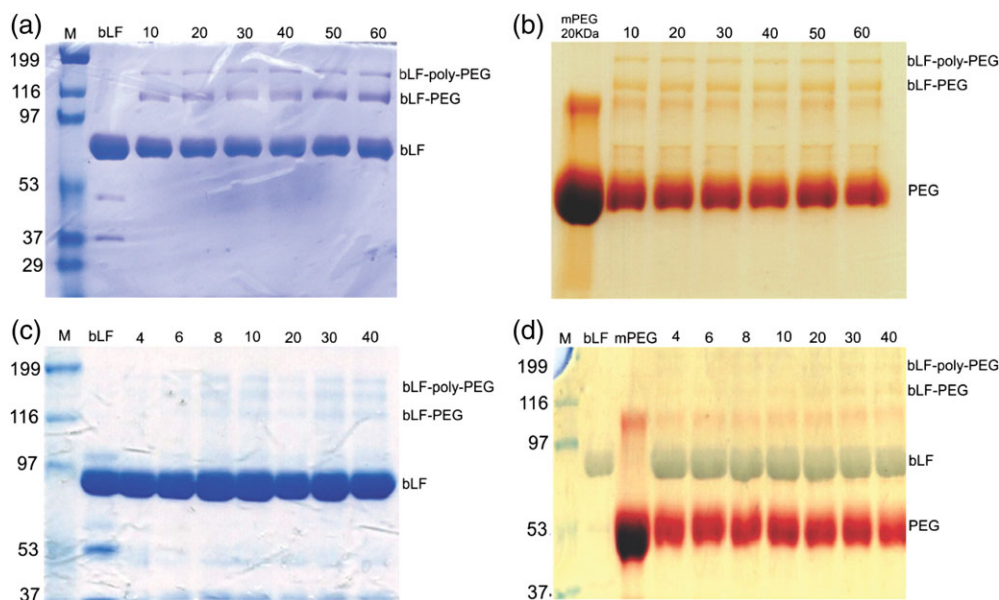


Figure 11. SDS-PAGE analyses of the bioconjugation reactions at different times (min) of bLF with **2** stained with (a) Coomassie Brilliant Blue and (b) I_3^- ; conjugation of bLF with **3b** stained with (c) Coomassie Brilliant Blue and (d) I_3^- . [Color figure can be viewed at wileyonlinelibrary.com]

Cumulative conversion of PEGylated bLF (mono-PEGylated + poly-PEGylated) is shown in Figure 12. For the construction of the graph presented in Figure 12, the concentration of PEG–bLF was arbitrarily set as 100%, when the yield of the PEGylated adducts reached 41% using reagent **2**.²⁹ Conversion of bLF to the PEGylated adducts was higher with **2** than with reagent **3**, especially at long reaction times (40 min). This result is not surprising and agrees with the higher reactivity found for compound **2** in the hydrolysis experiments. For reagents **2** and **3a**, the reaction reached a plateau after 40 min at a total protein conversion of 41 and 23%, respectively. Despite the difference in the reactivity obtained for **2** and **3a**, this result suggests that both reagents slowly decompose under alkaline aqueous conditions and therefore cannot lead to complete protein conjugation.

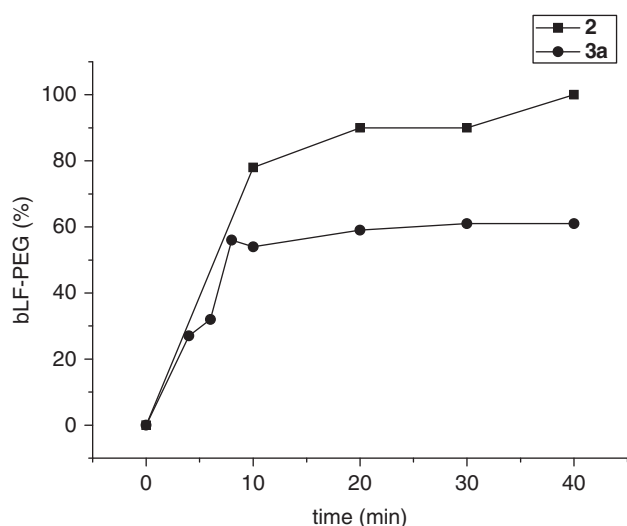


Figure 12. Profile of the PEGylation reaction of bLF with reagents (a) **2** and (b) **3a**

CONCLUSIONS

In this work, a simple methodology for the synthesis of mPEG–NHS carbonates bearing different alkyl spacers is presented. All products are obtained with high yields and purities. The kinetics of alkaline hydrolysis was used as a tool to evaluate the reactivity of the functional PEGs. On the basis of these experiments and supported by DFT calculations, a detailed mechanism for the hydrolysis reactions is proposed. We found that the stability of the carbonate increases significantly only when the length of the spacer was increased from 2 (compound **2**) to 3 (compound **3a**) carbon atoms, in clear contrast with the results published for mPEG–NHS esters. A further increase of the length of the spacer has only a limited effect on the stability of the reagent. An explanation for the change in the rate of the hydrolysis when moving from carbonates **2** to **3a** is provided by the difference in dimerization energies. On the contrary, a strong solvation effect was observed for NHS esters **1**. It is worth mentioning that the results obtained herein provide, for the first time, a rational explanation for the long-standing question of the effect of the lengths of alkyl spacers on the reactivity of important mPEG–NHS esters.

Finally, in the conjugation of bLF, we found that **3a** afforded lower cumulative yields of PEGylation than **2**, in agreement with the results obtained in the kinetic experiments.

ACKNOWLEDGMENTS

This work was supported by Consejo Nacional de Investigaciones Científica y Técnicas (CONICET) and Agencia Nacional de Promoción Científica y Tecnológica (ANPCyT) from Argentina. M. M. deeply acknowledges the receipt of an undergraduate fellowship from Universidad Nacional del Litoral (Cientibecas-UNL). We thank Dr. Javier F. Guastavino from INTEC for the synthesis of some of polymers **4**. The support to our work from Laboratorio Horian I+D is deeply acknowledged.

REFERENCES

1. Canalle, L. A.; Löwik, D. W. P. M.; von Hest, J. C. M. *Chem. Soc. Rev.* **2010**, 39, 329.
2. González, M.; Vaillard, S. E. *Curr. Org. Chem.* **2013**, 17, 975.
3. González, M.; Vaillard, S. E.; Grau, R. J. A. *Rec. Pat. Chem. Eng.* **2011**, 4, 241.
4. Ishihara, H. *Biol. Pharm. Bull.* **2013**, 36, 883.
5. Turecek, P. L.; Bossard, M. J.; Schoetens, F.; Ivens, I. A. *J. Pharm. Sci.* **2016**, 105, 460.
6. Veronese, F. M. *Biomaterials.* **2001**, 22, 405.
7. Jain, A. *Crit. Rev. Ther. Drug Carrier Syst.* **2015**, 32, 403.
8. Pasut, G.; Veronese, F. M. *Prog. Polym. Sci.* **2007**, 32, 933.
9. Damodaran, V. D.; Fee, C. J. *Eur. Pharm. Rev.* **2010**, 15, 18.
10. Roberts, M. J.; Bentley, M. D.; Harris, J. M. *Adv. Drug. Deliver. Rev.* **2002**, 54, 459.
11. Harris, J. M.; Kozlowski, A. U. S. Patent 5,672,662 (1997).
12. Bentley, M. D.; Zhao, X.; Shen, X.; Guo, L. U. S. Patent 7,674,879 (2010).
13. Guastavino, J. F.; Vaillard, V. A.; Cristaldi, M. D.; Rossini, L.; Vaillard, S. E. *Macromol. Chem. Phys.* **2016**, 217, 1745.
14. Neese, F. *Wiley Interdiscip. Rev.: Comput. Mol. Sci.* **2018**, 8, 1.
15. Perdew, J. P.; Burke, K.; Ernzerhof, M. *Phys. Rev. Lett.* **1996**, 77, 3865.
16. Weigend, F.; Ahlrichs, R. *Phys. Chem. Chem. Phys.* **2005**, 7, 3297.
17. Weigend, F. *Phys. Chem. Chem. Phys.* **2006**, 8, 1057.
18. Kruse, H.; Grimme, S. *J. Chem. Phys.* **2012**, 136, 154101.
19. Grimme, S.; Ehrlich, S.; Goerigk, L. *J. Comput. Chem.* **2011**, 32, 1456.
20. Grimme, S.; Jens, A.; Ehrlich, S.; Krieg, H. *J. Chem. Phys.* **2010**, 132, 154104.
21. Barone, V.; Cossi, M. *J. Phys. Chem. A.* **1998**, 102, 1995.
22. Ramón, J. A.; Peniche, C. *Quim. Nova.* **2009**, 32, 1426.
23. Zalipsky, S. *Bioconjugate Chem.* **1995**, 6, 150.
24. Wu, D.; Zhao, H.; Greewald, B. U. S. Patent 7,365,127 (2008).
25. Kim, S.-I.; Hwang, S.-J.; Jung, E.-M.; Um, I.-K. *Bull. Korean Chem. Soc.* **2010**, 31, 2015.
26. Marlier, J. F.; O'Leary, M. H. *J. Am. Chem. Soc.* **1990**, 112, 5996.
27. Klykov, O.; Weller, M. G. *Anal. Methods.* **2015**, 7, 6443.
28. Fox, J. M.; Dmitrenko, O.; Liao, L.-a.; Bach, R. D. *J. Org. Chem.* **2002**, 69, 7317.
29. Tomita, M.; Wakabayashi, H.; Yamauchi, K.; Teraguchi, S.; Hayasawa, H. *Biochem. Cell. Biol.* **2002**, 80, 109.
30. Yamauchi, K.; Wakabayashi, H.; Shin, K.; Takase, M. *Biochem. Cell Biol.* **2006**, 84, 291.
31. Mulder, A. M.; Connellan, P.A.; Oliver, C.J.; Morris, C. A.; Stevenson, L. M. *Nutr. Res.* **2008**, 28, 583.
32. Hutchens, T. W.; Rumball, S. V.; Lönerdal, B., Eds. *Lactoferrin: Structure and Function*; New York: Springer Science and Business Media, **1994**.
33. Kato, K.; Tamaki, N.; Saito, Y.; Fujimoto, T.; Sato, A. *Biol. Pharm. Bull.* **2010**, 33, 1253.
34. Nojima, Y.; Suzuki, Y.; Iguchi, K.; Shiga, T.; Iwata, A.; Fujimoto, T.; Yoshida, K.; Shimidzu, H.; Takeuchi, T.; Sato, A. *Bioconjugate Chem.* **2008**, 19, 2253.
35. Nojima, Y.; Suzuki, Y.; Yoshida, K.; Abe, F.; Shiga, T.; Takeuchi, T.; Sugiyama, A. *Pharm. Bull.* **2009**, 26, 2125.
36. Sugiyama, A.; Sato, A.; Takeuchi, T. *Food Chem. Toxicol.* **2009**, 47, 1453.
37. Nojima, Y.; Iguchi, K.; Suzuki, Y.; Sato, A. *Biol. Pharm. Bull.* **2009**, 32, 523.
38. Sugiyama, A.; Sato, A.; Shimizu, H.; Ando, K.; Takeuchi, T. *J. Vet. Med. Sci.* **2010**, 72, 173.